Molecular Imaging and Biology
DOI 10.1007/s11307-021-01660-7

RESEARCH ARTICLE

Amyloid-β PET Classification on Cognitive Aging Stages Using the Centiloid Scale

Giordana Salvi de Souza[1,2], Michele Alberton Andrade[1,2,3], Wyllians Vendramini Borelli[3], Lucas Porcello Schilling[3], Cristina Sebastião Matushita[3], Mirna Wetters Portuguez[1,3], Jaderson Costa da Costa[1,3], and Ana Maria Marques da Silva[1,2,3]

[1]*School of Medicine, PUCRS, Porto Alegre, Brazil*
[2]*Medical Image Computing Laboratory, School of Technology, PUCRS, Porto Alegre, Brazil*
[3]*Brain Institute of Rio Grande Do Sul (BraIns), PUCRS, Porto Alegre, Brazil 2021*

Abstract

Propose: This study aims to explore the use of the Centiloid (CL) method in amyloid-β PET quantification to evaluate distinct cognitive aging stages, investigating subjects' mismatch classification using different cut-points for amyloid-β positivity.

Procedures: The CL equation was applied in four groups of individuals: SuperAgers (SA), healthy age-matched controls (AC), healthy middle-aged controls (MC), and Alzheimer's disease (AD). The amyloid-β burden was calculated and compared between groups and quantitative variables. Three different cut-points (Jack CR, Wiste HJ, Weigand SD, et al., Alzheimer's Dement 13:205–216, 2017; Salvadó G, Molinuevo JL, Brugulat-Serrat A, et al., Alzheimer's Res Ther 11:27, 2019; and Amadoru S, Doré V, McLean CA, et al., Alzheimer's Res Ther 12:22, 2020) were applied in CL values to differentiate the earliest abnormal pathophysiological accumulation of Aβ and the established Aβ pathology.

Results: The AD group exhibited a significantly increased Aβ burden compared to the MC, but not AC groups. Both healthy control (MC and AC) groups were not significantly different. Visually, the SA group showed a diverse distribution of CL values compared with MC; however, the difference was not significant. The CL values have a moderate and significant relationship between Aβ visual read, RAVLT DR and MMSE. Depending on the cut-point used, 10 CL, 19 CL, or 30 CL, 7.5% of our individuals had a different classification in the Aβ positivity. For the AC group, we obtained about 40 to 60% of the individuals classified as positive.

Conclusion: SuperAgers exhibited a similar Aβ load to AC and MC, differing in cognitive performance. Independently of cut-point used (10 CL, 19 CL, or 30 CL), three SA individuals were classified as Aβ positive, showing the duality between the individual's clinics and the biological definition of Alzheimer's. Different cut-points lead to Aβ positivity classification mismatch in individuals, and an extra care is needed for individuals who have a CL value between 10 and 30 CL.

Key words Positron emission tomography · ^{11}C-PiB · Diagnostic imaging · Healthy aging · SuperAgers

Correspondence to: Giordana Salvi de Souza*; e-mail: giordana.souza@edu.pucrs.br*

Published online: 05 October 2021

Introduction

Human cognitive capacity reaches its peak in middle age, progressively decreasing after 50–60 years when a cognitive decline considered characteristically physiological occurs [1, 2]. In contrast to normal aging with a cognitive decline expected for age and education, brain aging could follow two other paths, successful or pathological aging. Successful aging is denominated by individuals 80 years or older who maintain memory ability similar to or superior to middle-aged subjects, named SuperAgers [3–7]. Pathological aging is mainly characterized by Alzheimer's disease (AD), with the presence of amyloid-β (Aβ), tau neurofibrillary tangles, and neurodegeneration.

The National Institute on Aging and Alzheimer's Association (NIA-AA), conceptualized as the [AT(N)] system, presents a new biomarker definition of AD, considering Aβ, pathologic tau, and neurodegeneration [8]. Various studies indicate that older adults with significant Aβ deposition are considered in a presymptomatic stage of Alzheimer's disease AD [9, 10]. In contrast, the International Working Group (IWG) (2021) argued that only the presence of Aβ and tau biomarkers are not sufficient to predict progression to prodromal AD or AD dementia confidently or to define a person's position on the AD continuum without clinical input [11].

Biomarkers have the potential to enhance diagnostic accuracy and facilitate the development of disease-modifying therapy [12]. In vivo fibrillar brain Aβ quantification is possible by using positron emission tomography (PET) imaging tracers as the ^{11}C-Pittsburgh Compound B (PIB) [13], ^{18}F-NAV4694 [14], ^{18}F-Florbetaben [15], ^{18}F-Flutemetamol [16], and ^{18}F-Florbetapir [17]. Thus, a precise assessment of Aβ biomarkers in the brain might be considered essential for improving the management of Aβ deposition and the effectiveness of treatment [18]. Still, a small number of treatment strategies targeting Aβ accumulation are available [19–23].

Different methods were proposed to process and analyze Aβ PET data, potentially reducing reproducibility and preventing comparison between studies [24]. The Centiloid scale (CL) was developed by the Centiloid Working Group to harmonize the acquisition protocol and quantification variability in Aβ PET. The CL approach standardizes the quantification of Aβ deposition by using PET data on a scale ranging from 0 to 100. The zero CL value represents the average uptake of the radiotracer in young individuals (< 34 years old), and the value of 100 represents the average uptake of individuals with AD.

Since its inception, the research community has gradually applied the CL method. Although it was initially conceived for the standardization of Aβ tracers analysis and the definition of the range of Aβ positivity characteristic of AD, other studies were conducted to correlate CL values with neuropathological results and Aβ plasma levels [25], in longitudinal cognitive evaluation [25, 26], or as a quantitative method in multicenter studies [27–34]. Moreover, the CL scale has also been applied for other diseases, such as Parkinson's disease [35], subcortical vascular dementia [36], chronic traumatic encephalopathy [37], and Down syndrome [38].

For diagnosis purposes, the development of approaches for the Aβ cut-point has received significant attention. In the last years, the studies published by Jack et al. [39], Salvadó et al. [40], and Amadoru et al. [41] provided different cut-points to differentiate the earliest abnormal pathophysiological accumulation of Aβ and the established Aβ pathology. Even knowing that the Aβ burden exists on a continuum, increasing the baseline may predict a corresponding increase in future cognitive decline rate [42]. Although the definition of a cut-point to establish the stage of Aβ accumulation is challenging due to the variability between different individuals, the lack of standardization and harmonization in cut-point values can cause a misclassification in the individuals.

The present work aims to investigate Aβ PET quantification on distinct cognitive aging stages, including the SuperAgers. We further explored the subject's classification using different cut-points for Aβ positivity, including the Centiloid method.

Materials and Methods

Participants

In this study, community-dwelling adults and elderly were invited to participate from January 2016 to March 2019 at the Brain Institute of Rio Grande do Sul. The Brazilian SuperAgers Cohort was designed to comprehend individuals from the extremes of the cognitive stages. Forty participants were included in this study, divided into four groups: SuperAgers (SA), age-matched controls (AC), middle-aged controls (MC), and Alzheimer's disease (AD). The SA group was defined based on previously described criteria [3, 4]: older adults at or above 80 years old with exceptional memory scores (delayed-recall scores above 1.5 SD for age and education) and standard scores for non-memory domains. The control groups were cognitively normal for age and education based on their age range, above 80 years old for the AC and between 55 and 65 years old for the MC. The older group was thought to have the same characteristics as the SuperAgers group—age and education to mitigate confounding factors. The AD group included individuals who matched the NIA-AA clinical criteria for dementia due to Alzheimer's disease [43].

All participants presented preserved activities of daily living, excluding the individuals with AD. The healthy cognitive individuals denied any family history of dementia or cognitive impairment. All individuals displayed negative scores for depression and anxiety when evaluated using the reduced Geriatric Depression Scale and the Beck Anxiety Inventory, respectively [44, 45]. The four groups were tested under a cognitive evaluation protocol that included the mini-mental state examination (MMSE) and the Rey auditory verbal learning test (RAVLT). Specifically, the delayed-recall memory

score (RAVLT DR) was applied because of its high predictive accuracy for progressive amnestic dementia [46]. Subsequently, they were examined under a neuroimaging protocol that included magnetic resonance (MR) imaging and ^{11}C-PiB PET. The university's ethical committee previously approved the study, and informed consent was obtained from all individual participants included in the study.

Sample Size

The sample size was calculated using the G * Power 3.1R program [47]. Based on the experimental design and previous experimental data [3], we calculated an effect size of F of 0.5647 (test details: significance (α) = 0.05, power ($1-\beta$ error probability) = 0.80, non-centrality parameter $\delta = 12.75$; critical = 2.8662; Df = 36; total sample number = 40; current power = 0.82). Based on the data presented above, the sample size was 10 individuals per group.

Imaging Acquisition

PET images were obtained using the ^{11}C-PiB tracer in a PET/CT Discovery D600 system (GE Healthcare, USA) in the three-dimensional scanning mode. The ^{11}C-PiB was injected into an antecubital vein as a bolus with a mean dose of 505 MBq (within a range of 307–762 MBq). PET scans were acquired in list mode, and static PET data were generated at 50–70 min after injection. CT scan was obtained for attenuation and scatter correction. Images were reconstructed by using the VUE Point HD (2 iterations, 32 subsets, a filter cutoff of 4.8 mm, a matrix size of 192 × 192 × 47, and a voxel size of 1.56 × 1.56 × 3.27 mm).

MR structural images were obtained using 3 T Signa HDxT equipment (GE Healthcare, USA) with an eight-channel head coil. Volumetric T1-weighted images were obtained by using the 3DBRAVO® sequence with a sagittal slice thickness of 1.0 mm (no gap), a repetition time (TR) of 6.272 ms, an echo time (TE) of 2.256 ms, a flip angle of 11°, a matrix size of 512 × 512 × 196, and a voxel size of 0.5 × 0.5 × 1.0 mm.

Image Processing

Klunk et al. provided the details of standardizing the PET-based Aβ burden quantification. The standard processing method is described by using the ^{11}C-PiB and MR images to implement the Centiloid scale.

The CL method is designed for measuring the "global" cortical Aβ deposition by using two volumes of interest (VOI): CTX (also called global cortical target region) and WC (whole cerebellum). The CTX VOI includes the typical brain regions with high Aβ load in AD, such as the frontal, temporal, parietal cortices, precuneus, anterior striatum, and insular cortex. The WC VOI represents a reference region because of its minimal Aβ deposition [24].

The image processing was performed on our site using the PMOD software package version 4.0 (PMOD LLC Technologies, Switzerland) with the PNEURO tool. The processing methodology was validated previously [48]. The Centiloid atlas (CTX and WC regions) is selected in the processing software, and then the PET and MR T1-weighted images are uploaded, reviewed, and re-orientated. The PET and MR images are co-registered and processed by using the maximum probability atlas analysis. The Centiloid atlas is applied, and the output is used to derive the standardized uptake value ratio (SUVR) for CTX and WC.

In addition, T1-weighted images of all participants were processed with the Computational Anatomy Toolbox (CAT) 12 (http://www.neuro.uni-jena.de/cat/, version r1109) within Statistical Parametric Mapping (SPM) 12 using MATLAB (12a). The estimation of cortical thickness in CAT is based on the PBT method and is fully automated, and we used the default settings described in detail in the manual of the CAT 12 toolbox.

Image Analysis

The level-1 Centiloid replication analysis was first performed as prescribed by Klunk et al. [24]. The Centiloid analysis implementation with GAAIN data presented a strong agreement with the previously published measurements ($R^2 = 0.999$). The fit exceeded the minimum specified acceptance criteria (slope = 0.9907; intercept = 0.0249).

Reproducing the image processing pipeline in our site with the GAAIN dataset, the CL equation is defined as follows:

$$\mathrm{CL} = 100(SUVR_{subject} - 1.008)/1.059.$$

This CL equation was applied in our study population for MC, AC, AD, and SA.

A scatter graph was plotted to calculate a linear regression and Pearson's correlation [24] to compare the CL results of the Centiloid study and the CL results processed in our institution. The data are presented in the Electronic Supplementary Material.

One Aβ PET expert reader (author CM), blinded to CL values and neuropathological data, visually interpreted all scans using the GE healthcare workstation (AW 4.6), as used in the clinical practice.

Amyloid-β Cut-Point

To evaluate how the Aβ cut-point classifies our individuals, we used the cut-points proposed by Jack et al. (2017) [39], Salvadó et al. (2019) [40], and Amadoru et al. (2020) [41]. Several studies have reported optimal CL cutoff values for Aβ positivity. Fig. 1 presents published cut-point values and shows their variability to define early and established Aβ accumulation [33, 39–41, 49–54]. Jack et al. defined a cut-point of 19 CL based on the reliable worsening cut-point. Salvadó et al. (2019) reported the optimal cut-point value of

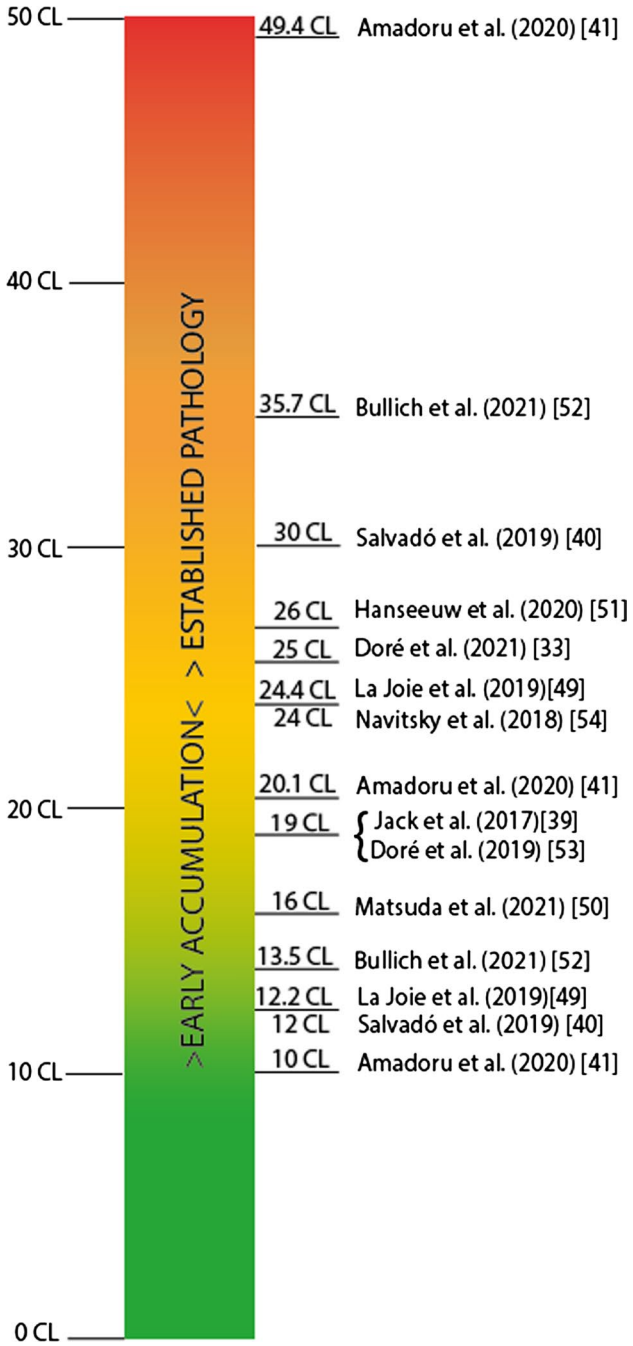

Fig. 1. Illustration of the published cut-point values for CL to divide the Aβ uptake as early accumulation (> 10 CL to < 24 CL) and established AD pathology (> 24 CL).

12 CL, which agrees with the values found for cerebrospinal fluid (CSF) $A\beta_{42}$ and 30 CL indicating the presence of established pathology by comparison with the phosphorylated tau/Aβ42 ratio or total tau/Aβ42 ratio of the CSF. Amadoru et al. (2020) defined an optimal cut-point of 10 CL, accurately reflecting the absence of any neuritic plaque, 20 CL indicates the presence of moderate plaque density, and approximately 50 CL or more is confirmed by both neuropathological and clinicopathological diagnosis of AD.

Table 1. Demographic and clinical information in terms of the mean and SD of participants in our study

	MC ($n=10$)	AC ($n=10$)	SA ($n=10$)	AD ($n=10$)	p value[b]
Age	58.70 (5.52)	83.5 (4.22)	82.3 (2.63)	78.2 (6.14)	< 0.001
Gender (F/M)	9/1	7/3	7/3	5/5	0.302
Education	14.6 (4.79)	12.9 (4.98)	12.7 (4.79)	14.5 (5.40)	0.745
MMSE	29.6 (0.70)	27.9 (1.20)	28.6 (1.26)	22.0 (5.58)	< 0.001
RAVLT DR-	10.5 (3.21)	6.9 (1.60)	11.4 (2.01)	0.38 (0.52)[a]	< 0.001

[a]Calculated only for eight participants

[b]Group differences evaluated with ANOVA test

Abbreviations: *MC* middle-aged controls, *AC* age-matched controls, *SA* SuperAgers, *AD* Alzheimer's disease, *MMSE* mini mental state examination, *RAVLT DR* Rey auditory verbal learning test—delayed-recall memory scores

Statistical Analysis

The statistical analysis was performed in the IBM SPSS software, version 24.0 (Armonk, NY). Pearson's correlation coefficients and linear regressions were calculated for the SUVR and the CL scale using the GAAIN dataset and to compare the CL scale with other quantitative variables. The normality of the distributions was tested using the Shapiro–Wilk test. Demographic and quantitative variables were compared between groups with ANOVA, followed by Tukey's post hoc test. It was considered an $\alpha = 0.05$. The multiple comparisons were corrected by Bonferroni method. The effect size was calculated using Cohen's d. Data are presented as means ± standard deviation unless otherwise stated. As the CL is a linear transformation of SUVR, the discussion will be presented in terms of CL. The general linear model was employed to compare CL with clinical variables (RAVLT DR and MMSE), education, and age among the groups.

Results

Demographics

A total of 40 participants were included in our study (Table 1). There were no significant differences in age or gender between the groups. As expected by the inclusion criteria for age, the MC group was significantly different between AC, SA, and AD groups ($p < 0.001$, corrected). Significantly lower MMSE scores were observed in the AD group compared with other groups ($p < 0.001$, corrected). The MC, AC, and SA participants showed high RAVLT DR scores when compared with AD ($p < 0.001$, corrected), and the AC group differed significantly from the MC and SA groups ($p = 0.003$ and $p < 0.001$ corrected, respectively).

Amyloid-β Quantification and Visual Read

The summary of the CL results for all groups is shown in Table 2. The effect sizes were large enough (Cohen's $d > 0.8$) to show consistent group differences, excluding the comparison between SA and MC groups. The SA group showed the highest range for the CL analyses, followed by the AC group. As expected, the AD group showed a significantly high Aβ burden for the CL method when compared with the MC ($d = 4.84$, $p < 0.001$, corrected), the SA group ($d = 1.77$, $p < 0.001$, corrected), and the AC group ($d = 1.61$, $p = 0.005$, corrected). The Aβ load of the SA group did not differ significantly from the two control groups (MC and AC groups) ($d = 0.74$, $p = 0.665$; $d = 1.25$, $p = 1.00$, corrected, respectively), and the MC and the AC groups did not differ significantly from each other ($d = 1.61$, $p = 0.05$, corrected). All pairwise statistical comparisons are presented in the Electronic Supplementary Material, Table S1.

Correlation of CL values with Aβ PET expert visual read (negative or positive) obtained a significant moderate relationship with a value of $r = 0.639$ and $p < 0.001$. Five participants had a positive global uptake but a negative quantification (< 10 CL), and one participant had CL above 30 with visual assessment negative.

Cortical Thickness and CL Values

The summary of the cortical thickness results for all groups is shown in Table 3. The cortical thickness values are significantly different among the groups ($p < 0.001$). The MC group has a significantly high cortical thickness compared with the AC ($d = 3.34$, $p = 0.001$, corrected), the SA group ($d = 2.57$, $p < 0.001$, corrected), and the AD group ($d = 2.36$, $p < 0.001$, corrected). The AC, SA, and AD groups are not significantly different in cortical thickness. All pairwise statistical comparisons are presented in the Electronic Supplementary Material, Table S1.

There is a moderate negative linear correlation between CL values and cortical thickness with $r = -0.322$ and $p < 0.001$. Fig. 2 shows how the distribution of cortical thickness values among the groups. The MC group has the highest range between the minimum and maximum cortical thickness values (2.51 mm and 2.72 mm). The AC group presents a very similar cortical thickness among the participants, even though they vary on the CL scale. The SA group has a higher variation and lower cortical thickness values than the same age group (AC). Still, the SA individuals with higher CL values have higher cortical thickness values. Finally, the AD group has the smallest range between the minimum and maximum values, with a wide distribution of cortical thickness values.

Centiloid Scale and Neuropathological Variables

Both cognitive variables (RAVLT DR and MMSE) showed a strong negative relationship with CL values ($r = -0.561$, $p < 0.001$; $r = -0.457$, $p = 0.003$, respectively), presented

Table 2. Summary of the SUVR and CL results of our sample participants

	MC ($n = 10$)			AC ($n = 10$)			SA ($n = 10$)			AD ($n = 10$)			p value[a]
	Mean ± SD	CI (95%)	Range	Mean ± SD	CI (95%)	Range	Mean ± SD	CI (95%)	Range	Mean ± SD	CI (95%)	Range	
SUVR	1.01 ± 0,60*	0.96–1.05	0.95–1.16	1.35 ± 0.38	1.07–1.62	0.93–2.03	1.24 ± 0.44 *	0.92–1.55	0.91–2.28	1.86 ± 0.24	1.69–2.03	1.49–2.33	< 0.001
CL	− 0.18 ± 5.70*	− 4.26–3.89	− 5.63–14.71	31.96 ± 25.14	6.20–57.72	7.11–96.84	21.59 ± 41.15	− 7.85–51.02	− 9.11–119.87	80.43 ± 22.94	64.02–96.83	45.27–124.83	< 0.001

Abbreviations: *MC* middle-aged controls, *AC* age-matched controls, *SA* SuperAgers, *AD* Alzheimer's disease, *CI* confidence interval

[a]Group differences evaluated with ANOVA test

Table 3. Summary of the cortical thickness of our sample participants

	MC ($n=10$)	AC ($n=10$)	SA ($n=10$)	AD ($n=10$)	p value[a]
Cortical thickness	2.59 ± 0.06	2.4 ± 0.05	2.35 ± 0.1	2.32 ± 0.15	< 0.001

Abbreviations: *MC* middle-aged controls, *AC* age-matched controls, *SA* SuperAgers, *AD* Alzheimer's disease, *CI* confidence interval

[a]Group differences were evaluated with the ANOVA test

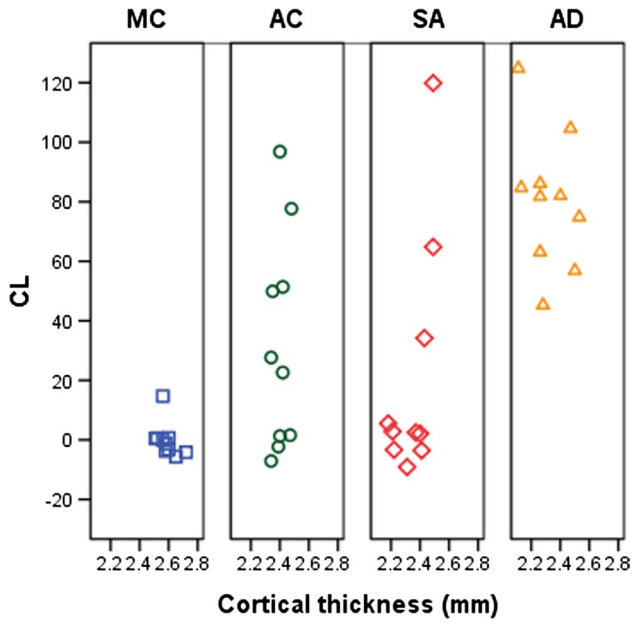

Fig. 2. Distribution of CL values and cortical thickness, in mm, for each group. The symbols represent the groups: MC, blue square; AC, green circle; SA, red diamond; AD, orange triangle.

in Fig. 3A, B. For comparison between CL vs age (Fig. 3C), a moderate and significative correlation ($r=0.32$, $p=0.043$) was obtained. However, for the CL vs education, it was obtained a negligible relationship and no significance ($r=-0.100$, $p=0.541$) as shown in Fig.3D.

As shown in Fig. 4, the individuals were divided into three groups: low Aβ uptake (< 10CL); low-intermediate Aβ uptake (> 10 CL and < 30 CL); and intermediate-high Aβ uptake (> 30 CL). It was observed that younger individuals (between 50 and 60 years old) who have low Aβ uptake perform optimally on the RAVLT DR test, and with advancing age, this performance regresses. Most individuals with > 30 CL perform worse on the test, regardless of age. Few individuals showed a low-intermediate Aβ uptake. Interestingly, there are two individuals with similar age and identical RAVLT DR scores in the opposite group, one from the < 10 CL group and the other from the > 30 CL group. Surprisingly, both individuals are classified as SuperAgers.

Amyloid-β Classification in the Clinical Setting

Fig. 5 presents our sample participants' CL values distribution, which shows their positioning for different cut-point values. Regardless of the cut-point chosen, the AD individuals were above the three cut-point used (the minimum CL value of AD patients was 45.3). Aβ positivity differed from each cut-point used in MC, AC, and SA. Using 10 CL as cut-point (Amadoru et al. 2020), one MC, six AC, and three SA were classified as Aβ-positive. Using the low-intermediate value of 19 CL presented by Jack et al., six AC and three SA were classified as Aβ positive. Considering an intermediate value of 30 CL [40], four AC and three SA were classified as Aβ positive.

Discussion

To our knowledge, this study represents the first report that sought to evaluate different degrees of successful cognitive stages using the Centiloid scale, from normal aging to SuperAgers. Analyzing the distribution of individuals with different aging stages on the CL allowed the investigation of how the use of different cut-points for the Aβ classification might impact the diagnosis of AD pathology.

It is expected that 30% of clinically normal elderly individuals have AD at autopsy or a high Aβ burden [55–57]. In our sample, 60% of the AC group showed a CL value above 10 CL, and 40% of the AC group showed a CL value above 30 CL. The AC group presented variable values of CL, from − 7.11 to 96.84 (mean, 31.96 ± 25.14 CL). The other healthy group, the MC group, showed a low Aβ uptake, with a mean value of − 0.18 ± 5.70 CL, which was expected for their age. In addition, the MC group differed significantly from the AD group and was not significantly different from the AC group. The CL values and Aβ visual read obtained a significant moderate relationship with $r=0.639$ and $p<0.001$. When considering visual reading, there are rare cases of clear focal Aβ uptake that can lead to a positive visual read, and perhaps this is what happened to the five individuals with low Aβ uptake who were classified as positive. Also, the CL scale obtained moderate to strong correlations with analyzed variables such as education, MMSE, RAVLT DR, cortical thickness, and all proportionally inverse, as showed in a similar study [58–60].

As expected, the CL values of SuperAgers were significantly different compared with the AD group. Previous studies have shown that SuperAgers can exhibit positivity in Aβ, comparable to age peers [3, 61, 62], which aligns with our results. Visually, the SA group showed a different distribution of CL values compared with the MC group; however, the difference was not statistically significant, although there is a statistical difference between the cortical thicknesses. The SA and AC groups visually presented a similar distribution, with some individuals showing high values of CL and others low CL values. Independently of cut-point, three SA

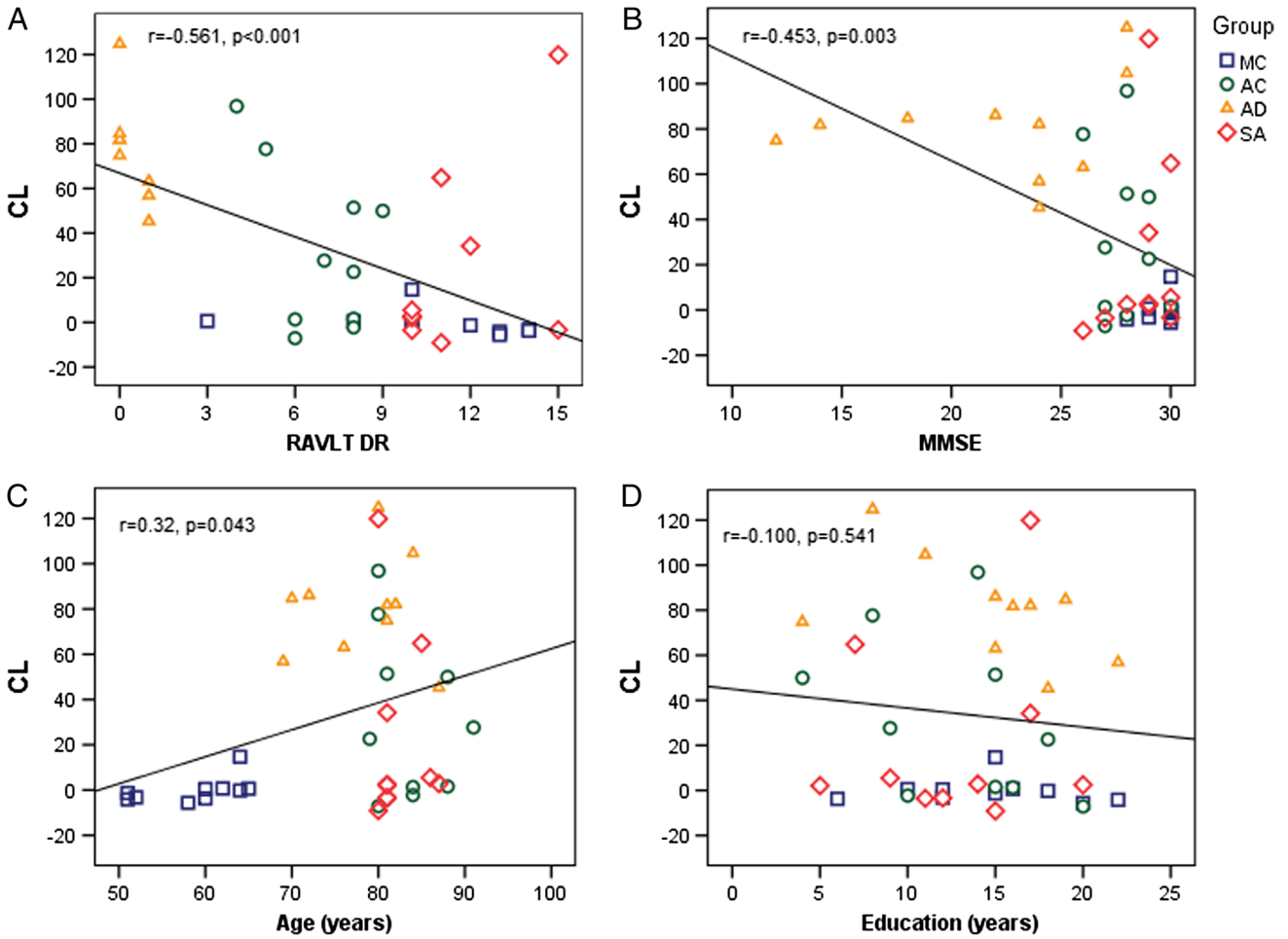

Fig. 3. Scatter graphs of correlations between CL values and clinical variables. **A** Comparison between CL values and RAVLT DR. **B** Comparison between CL values and MMSE. **C** Comparison between CL values and education. **D** Comparison between CL values and age.

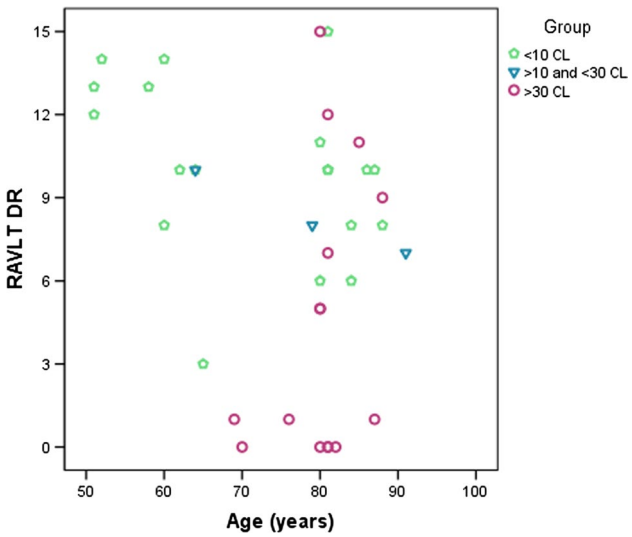

Fig. 4. Scatter graphs of correlations between RAVLT DR and age, separated by the groups of CL values below 10 CL, values between 10 and 30 CL, and above 30 CL. The symbols represent the groups: green pentagon, < 10 CL; blue inverted triangle, > 10 and < 30 CL; purple circle, > 30 CL.

individuals were classified as Aβ positive (Fig. 5) [39–41], showing values above 30 CL (34.2 CL, 64.83 CL, and 119.87 CL). According to Salvadó et al. (2019), a value above 30 CL indicates the presence of established AD pathology. Fig. 4 shows the duality between the individual's clinics and the biological definition of Alzheimer's, and that the presence of Aβ plaques does not interfere with an individual's cognitive performance. Nevertheless, using only the cut-point for the Aβ classification of the individual, some SA would be classified as a prodromal AD [8]. However, when their age and the high capacity in the cognitive tests and routine performances are considered, they are not. One hypothesis about SuperAgers performance is that they are resilient to cognitive decline despite increasing age [4, 62, 63].

A single cut-point for Aβ positivity is highly desired for interpreting Aβ PET imaging studies and classifying the patient at a specific time [8]. However, Fig. 5 shows that a single cut-point might fail to classify some individuals. In our sample, we observed a classification mismatch in 7.5% of individuals evaluated (one MC and two AC subjects).

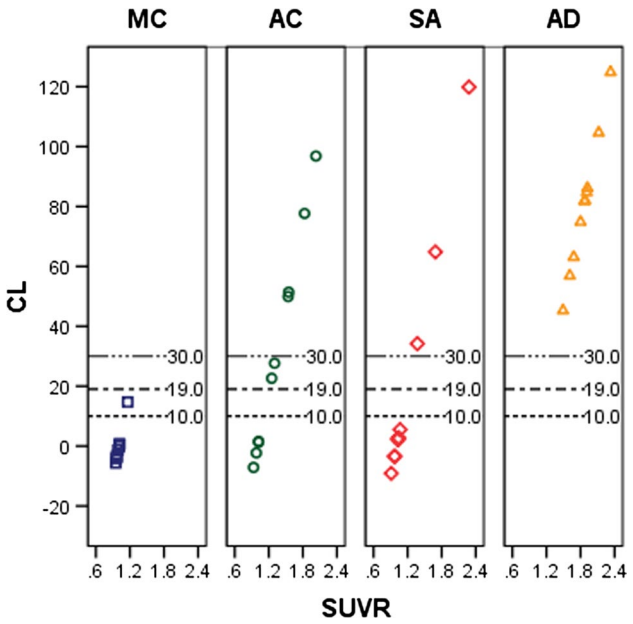

Fig. 5. Scatter graphs of CL distributions, separated by the cut-points of 10 CL, 19 CL, and 30 CL. The symbols represent the groups: blue square, MC group; green circle, AC group; red diamond, SA group; orange triangle, AD group.

Therefore, our suggestion for improving the clinical classification of the Aβ burden is using the cut-points as a reference for continuum classification. The lowest value classifies any neuritic plaque (< 10–12 CL), a middle-range value classifies early Aβ deposition (12–24 CL), and the highest confirms the presence of AD pathology (> 24 CL). Also, reporting the individual's Centiloid value is a reliable manner to monitor the Aβ accumulation in the brain longitudinally. Moreover, although pre-clinical evaluation of Aβ positivity is not recommended by the IWG [11], we believe that individuals who have an early Aβ deposition without a clinical diagnosis might benefit from early therapy and prevention strategies.

Despite our efforts, this study has some limitations. The small sample size cannot represent the general population, and its generalization must be interpreted cautiously. Additionally, it was not possible to evaluate the tau deposition in our sample. The use of tau information as a biomarker has been increasing in practice because it reflects the intensity of neuronal damage and tracking disease progression and is endorsed by NIA-AA in the AT[N] system [8] and by IWG recommendation [11]. Further analysis should consider tau biomarkers' use in investigating cognitive decline and harmonizing the cut-point values to classify individuals according to the CL values.

Conclusion

SuperAgers exhibited a similar Aβ load to that of age-matched healthy controls and middle-aged controls. However, independently of the cut-point used (10 CL, 19 CL, or 30 CL), three SA individuals were classified as Aβ positive. Also, different cut-points proposed for the CL determined a classification mismatch in 7.5% of individuals evaluated in this study. As the CL has been increasingly used in randomized clinical trials, more studies need to be developed to harmonize cut-point values.

For clinical diagnosis, special attention is required for individuals with a CL value between 10 and 30 CL because the Aβ burden is undeniably a decisive risk factor for adverse cognitive outcomes. As recommended by IWG (2021), the AD diagnosis must consider biological patterns and clinical symptoms. Also, Aβ imaging techniques should be carefully addressed, standardized, and interpreted in clinical settings.

Supplementary Information The online version contains supplementary material available at https://doi.org/10.1007/s11307-021-01660-7.

Funding This work was supported by CNPq [grant number 403029/2016–3], FAPERGS [grant number 27971.414.15498.22062017], and in part by CAPES [Finance Code 001].

Declarations

Conflict of Interest The authors declare that they have no conflict of interest.

References

1. Bishop NA, Lu T, Yankner BA (2010) Neural mechanisms of ageing and cognitive decline. Nature 464:529–535. https://doi.org/10.1038/nature08983
2. Morrison JH, Baxter MG (2012) The ageing cortical synapse: hallmarks and implications for cognitive decline. Nat Rev Neurosci 13:240–250. https://doi.org/10.1038/nrn3200
3. Harrison TM, Weintraub S, Mesulam M-M, Rogalski E (2012) Superior memory and higher cortical volumes in unusually successful cognitive aging. J Int Neuropsychol Soc 18:1081–1085. https://doi.org/10.1017/S1355617712000847
4. Borelli WV, Carmona KC, Studart-Neto A et al (2018) Operationalized definition of older adults with high cognitive performance. Dement Neuropsychol 12:221–227. https://doi.org/10.1590/1980-57642018dn12-030001
5. Borelli WV, Schilling LP, Radaelli G et al (2018) Neurobiological findings associated with high cognitive performance in older adults: a systematic review. Int Psychogeriatr 30:1813–1825. https://doi.org/10.1017/S1041610218000431
6. Alzheimer's Disease Neuroimaging Initiative, Baran TM, Lin FV (2018) Amyloid and FDG PET of successful cognitive aging: global and cingulate-specific differences. J Alzheimers Dis 66:307–318. https://doi.org/10.3233/JAD-180360
7. Calandri IL, Crivelli L, Martin ME et al (2020) Environmental factors between normal and superagers in an Argentine cohort. Dement Neuropsychol 14:345–349. https://doi.org/10.1590/1980-57642020dn14-040003
8. Jack CR, Bennett DA, Blennow K et al (2018) NIA-AA research framework: toward a biological definition of Alzheimer's disease. Alzheimer's Dement 14:535–562. https://doi.org/10.1016/j.jalz.2018.02.018
9. Caselli RJ, Reiman EM (2012) Characterizing the preclinical stages of Alzheimer's disease and the prospect of presymptomatic intervention. J Alzheimers Dis 33:S405–S416. https://doi.org/10.3233/JAD-2012-129026
10. Jessen F, Amariglio RE, Buckley RF et al (2020) The characterisation of subjective cognitive decline. Lancet Neurol 19:271–278. https://doi.org/10.1016/S1474-4422(19)30368-0
11. Dubois B, Villain N, Frisoni GB, et al (2021) Clinical diagnosis of Alzheimer's disease: recommendations of the International Working Group. Lancet Neurol. https://doi.org/10.1016/S1474-4422(21)00066-1

12. Khoury R, Ghossoub E (2019) Diagnostic biomarkers of Alzheimer's disease: a state-of-the-art review. Biomark Neuropsychiatry 1:100005. https://doi.org/10.1016/j.bionps.2019.100005
13. Klunk WE, Engler H, Nordberg A et al (2004) Imaging brain amyloid in Alzheimer's disease with Pittsburgh Compound-B: imaging amyloid in AD with PIB. Ann Neurol 55:306–319. https://doi.org/10.1002/ana.20009
14. Rowe CC, Pejoska S, Mulligan RS et al (2013) Head-to-head comparison of 11C-PiB and 18F-AZD4694 (NAV4694) for β-amyloid imaging in aging and dementia. J Nucl Med 54:880–886. https://doi.org/10.2967/jnumed.112.114785
15. Rowe CC, Ackerman U, Browne W et al (2008) Imaging of amyloid β in Alzheimer's disease with 18F-BAY94-9172, a novel PET tracer: proof of mechanism. Lancet Neurol 7:129–135. https://doi.org/10.1016/S1474-4422(08)70001-2
16. Serdons K, Verduyckt T, Vanderghinste D et al (2009) Synthesis of 18F-labelled 2-(4′-fluorophenyl)-1,3-benzothiazole and evaluation as amyloid imaging agent in comparison with [11C]PIB. Bioorg Med Chem Lett 19:602–605. https://doi.org/10.1016/j.bmcl.2008.12.069
17. Wong DF, Rosenberg PB, Zhou Y et al (2010) In vivo imaging of amyloid deposition in Alzheimer disease using the radioligand 18F-AV-45 (Flobetapir F 18). J Nucl Med 51:913–920. https://doi.org/10.2967/jnumed.109.069088
18. Cummings J (2019) The role of biomarkers in Alzheimer's disease drug development. Adv Exp Med Biol 1118:29–61. https://doi.org/10.1007/978-3-030-05542-4_2
19. Aisen PS (2009) Alzheimer's disease therapeutic research: the path forward. Alzheimer Res Ther 1:2. https://doi.org/10.1186/alzrt2
20. Aisen PS, Andrieu S, Sampaio C et al (2011) Report of the task force on designing clinical trials in early (predementia) AD. Neurology 76:280–286. https://doi.org/10.1212/WNL.0b013e318207b1b9
21. Doody RS, Raman R, Farlow M et al (2013) A phase 3 trial of semagacestat for treatment of Alzheimer's disease. N Engl J Med 369:341–350. https://doi.org/10.1056/NEJMoa1210951
22. Huang Y, Mucke L (2012) Alzheimer mechanisms and therapeutic strategies. Cell 148:1204–1222. https://doi.org/10.1016/j.cell.2012.02.040
23. Ferrero J, Williams L, Stella H et al (2016) First-in-human, double-blind, placebo-controlled, single-dose escalation study of aducanumab (BIIB037) in mild-to-moderate Alzheimer's disease. Alzheimer's & Dementia: Translational Research & Clinical Interventions 2:169–176. https://doi.org/10.1016/j.trci.2016.06.002
24. Klunk WE, Koeppe RA, Price JC et al (2015) The Centiloid project: standardizing quantitative amyloid plaque estimation by PET. Alzheimer's Dement 11:1-15.e4. https://doi.org/10.1016/j.jalz.2014.07.003
25 Burnham SC, Fandos N, Fowler C et al (2020) Longitudinal evaluation of the natural history of amyloid-β in plasma and brain. Brain Commun 2(1):fcaa041. https://doi.org/10.1093/braincomms/fcaa041
26. Su Y, Flores S, Wang G et al (2019) Comparison of Pittsburgh compound B and florbetapir in cross-sectional and longitudinal studies. Alzheimer's Dement Diagn Assess Dis Monit 11:180–190. https://doi.org/10.1016/j.dadm.2018.12.008
27. Lopes Alves I, Collij LE, Altomare D, al, et al (2020) Quantitative amyloid PET in Alzheimer's disease: the AMYPAD prognostic and natural history study. Alzheimer's Dement 16:750–758. https://doi.org/10.1002/alz.12069
28. Callahan CM, Apostolova LG, Gao S et al (2020) Novel markers of angiogenesis in the setting of cognitive impairment and dementia. J Alzheimers Dis 75:959–969. https://doi.org/10.3233/JAD-191293
29. Risacher SL, Fandos N, Romero J et al (2019) Plasma amyloid beta levels are associated with cerebral amyloid and tau deposition. Alzheimer's Dement Diagn Assess Dis Monit 11:510–519. https://doi.org/10.1016/j.dadm.2019.05.007
30. Risacher SL, Tallman EF, West JD et al (2017) Olfactory identification in subjective cognitive decline and mild cognitive impairment: association with tau but not amyloid positron emission tomography. Alzheimer's Dement Diagn Assess Dis Monit 9:57–66. https://doi.org/10.1016/j.dadm.2017.09.001
31. Pappas C, Klinedinst BS, Le S, et al (2020) CSF glucose tracks regional tau progression based on Alzheimer's disease risk factors. Alzheimer's Dement Transl Res Clin Interv 6 https://doi.org/10.1002/trc2.12080
32. Thirunavu V, McCullough A, Su Y et al (2019) Higher body mass index is associated with lower cortical amyloid-β burden in cognitively normal individuals in late-life. J Alzheimers Dis 69:817–827. https://doi.org/10.3233/JAD-190154
33. Doré V, Krishnadas N, Huang K, et al (2021) Relationship between amyloid and tau levels and its impact on tau spreading. Eur J Nucl Med Mol Imaging 8 https://doi.org/10.1007/s00259-021-05191-9
34. Klein G, Delmar P, Voyle N et al (2019) Gantenerumab reduces amyloid-β plaques in patients with prodromal to moderate Alzheimer's disease: a PET substudy interim analysis. Alzheimer's Res Ther 11:101. https://doi.org/10.1186/s13195-019-0559-z
35. Melzer TR, Stark MR, Keenan RJ et al (2019) Beta amyloid deposition is not associated with cognitive impairment in Parkinson's disease. Front Neurol 10:391. https://doi.org/10.3389/fneur.2019.00391
36. Yun HJ, Moon SH, Kim HJ et al (2017) Centiloid method evaluation for amyloid PET of subcortical vascular dementia. Sci Rep 7:16322. https://doi.org/10.1038/s41598-017-16236-1
37. Lesman-Segev OH, La Joie R, Stephens ML et al (2019) Tau PET and multimodal brain imaging in patients at risk for chronic traumatic encephalopathy. NeuroImage Clin 24:102025. https://doi.org/10.1016/j.nicl.2019.102025
38. Zammit MD, Laymon CM, Betthauser TJ, et al (2020) Amyloid accumulation in Down syndrome measured with amyloid load. Alzheimer's Dement 12 https://doi.org/10.1002/dad2.12020
39. Jack CR, Wiste HJ, Weigand SD et al (2017) Defining imaging biomarker cut points for brain aging and Alzheimer's disease. Alzheimer's Dement 13:205–216. https://doi.org/10.1016/j.jalz.2016.08.005
40. Salvadó G, Molinuevo JL, Brugulat-Serrat A et al (2019) Centiloid cut-off values for optimal agreement between PET and CSF core AD biomarkers. Alzheimer's Res Ther 11:27. https://doi.org/10.1186/s13195-019-0478-z
41. Amadoru S, Doré V, McLean CA et al (2020) Comparison of amyloid PET measured in Centiloid units with neuropathological findings in Alzheimer's disease. Alzheimer's Res Ther 12:22. https://doi.org/10.1186/s13195-020-00587-5
42. Sperling RA, Donohue MC, Raman R et al (2020) Association of factors with elevated amyloid burden in clinically normal older individuals. JAMA Neurol 77:11. https://doi.org/10.1001/jamaneurol.2020.0387
43. McKhann GM, Knopman DS, Chertkow H et al (2011) The diagnosis of dementia due to Alzheimer's disease: recommendations from the National Institute on Aging-Alzheimer's Association workgroups on diagnostic guidelines for Alzheimer's disease. Alzheimer's Dement 7:263–269. https://doi.org/10.1016/j.jalz.2011.03.005
44. Yesavage JA, Sheikh JI (1986) Geriatric depression scale (GDS): recent evidence and development of a shorter version. Clin Gerontol 5:165–173. https://doi.org/10.1300/J018v05n01_09
45. Wang Y-P, Andrade LH, Gorenstein C (2005) Validation of the Beck depression inventory for a Portuguese-speaking Chinese community in Brazil. Braz J Med Biol Res 38:399–408. https://doi.org/10.1590/S0100-879X2005000300011
46. Knopman DS, Ryberg S (1989) A verbal memory test with high predictive accuracy for dementia of the Alzheimer type. Arch Neurol 46:141–145. https://doi.org/10.1001/archneur.1989.00520380041011
47. Faul F, Erdfelder E, Lang A-G, Buchner A (2007) G*Power 3: a flexible statistical power analysis program for the social, behavioral, and biomedical sciences. Behav Res Methods 39:175–191. https://doi.org/10.3758/BF03193146
48. Battle MR, Pillay LC, Lowe VJ et al (2018) Centiloid scaling for quantification of brain amyloid with [18F]flutemetamol using multiple processing methods. EJNMMI Res 8:107. https://doi.org/10.1186/s13550-018-0456-7
49. La Joie R, Ayakta N, Seeley WW et al (2019) Multisite study of the relationships between antemortem [11C]PIB-PET Centiloid values and postmortem measures of Alzheimer's disease neuropathology. Alzheimer's Dement 15:205–216. https://doi.org/10.1016/j.jalz.2018.09.001
50. Matsuda H, Ito K, Ishii K et al (2021) Quantitative evaluation of 18F-Flutemetamol PET in patients with cognitive impairment and suspected alzheimer's disease: a multicenter study. Front Neurol 11:578753. https://doi.org/10.3389/fneur.2020.578753
51. Hanseeuw BJ, Malotaux V, Dricot L et al (2021) Defining a Centiloid scale threshold predicting long-term progression to dementia in patients attending the memory clinic: an [18F] flutemetamol amyloid

PET study. Eur J Nucl Med Mol Imaging 48:302–310. https://doi.org/10.1007/s00259-020-04942-4
52. Bullich S, Roé-Vellvé N, Marquié M et al (2021) Early detection of amyloid load using 18F-florbetaben PET. Alz Res Therapy 13:67. https://doi.org/10.1186/s13195-021-00807-6
53. Doré V, Bullich S, Rowe CC et al (2019) Comparison of 18F-florbetaben quantification results using the standard Centiloid, MR-based, and MR-less CapAIBL® approaches: validation against histopathology. Alzheimer's Dement 15:807–816. https://doi.org/10.1016/j.jalz.2019.02.005
54. Navitsky M, Joshi AD, Kennedy I et al (2018) Standardization of amyloid quantitation with florbetapir standardized uptake value ratios to the Centiloid scale. Alzheimer's Dement 14:1565–1571. https://doi.org/10.1016/j.jalz.2018.06.1353
55. Okamura N, Furumoto S, Fodero-Tavoletti MT et al (2014) Non-invasive assessment of Alzheimer's disease neurofibrillary pathology using 18F-THK5105 PET. Brain 137:1762–1771. https://doi.org/10.1093/brain/awu064
56. Jansen WJ, Ossenkoppele R, Knol DL et al (2015) Prevalence of cerebral amyloid pathology in persons without dementia: a meta-analysis. JAMA 313:1924. https://doi.org/10.1001/jama.2015.4668
57. Chételat G, La Joie R, Villain N et al (2013) Amyloid imaging in cognitively normal individuals, at-risk populations and preclinical Alzheimer's disease. NeuroImage Clin 2:356–365. https://doi.org/10.1016/j.nicl.2013.02.006
58. Timmers T, Ossenkoppele R, Verfaillie SCJ et al (2019) Amyloid PET and cognitive decline in cognitively normal individuals: the SCIENCe project. Neurobiol Aging 79:50–58. https://doi.org/10.1016/j.neurobiolaging.2019.02.020
59. Villemagne VL, Pike KE, Chételat G et al (2011) Longitudinal assessment of Aβ and cognition in aging and Alzheimer's disease. Ann Neurol 69:181–192. https://doi.org/10.1002/ana.22248
60. Duara R, Loewenstein DA, Lizarraga G et al (2019) Effect of age, ethnicity, sex, cognitive status and APOE genotype on amyloid load and the threshold for amyloid positivity. NeuroImage Clin 22:101800. https://doi.org/10.1016/j.nicl.2019.101800
61. Dekhtyar M, Papp KV, Buckley R et al (2017) Neuroimaging markers associated with maintenance of optimal memory performance in late-life. Neuropsychologia 100:164–170. https://doi.org/10.1016/j.neuropsychologia.2017.04.037
62. Borelli WV, Leal-Conceição E, Andrade MA, et al (2021) Increased glucose activity in subgenual anterior cingulate and hippocampus of high performing older adults, despite amyloid burden. J Alzheimers Dis 1–10. https://doi.org/10.3233/JAD-210063
63. Gefen T, Shaw E, Whitney K et al (2014) Longitudinal neuropsychological performance of cognitive SuperAgers. J Am Geriatr Soc 62:1598–1600. https://doi.org/10.1111/jgs.12967